Colloids and Surfaces B: Biointerfaces 125 (2015) 255–263

Contents lists available at ScienceDirect

Colloids and Surfaces B: Biointerfaces

journal homepage: www.elsevier.com/locate/colsurfb

Antimicrobial surfaces containing cationic nanoparticles: How immobilized, clustered, and protruding cationic charge presentation affects killing activity and kinetics

Bing Fang[a], Ying Jiang[b], Klaus Nüsslein[c], Vincent M. Rotello[b], Maria M. Santore[a,*]

[a] Department of Polymer Science and Engineering, University of Massachusetts, Amherst, MA 01003, United States
[b] Department of Chemistry, University of Massachusetts, Amherst, MA 01003, United States
[c] Department of Microbiology, University of Massachusetts, Amherst, MA 01003, United States

ARTICLE INFO

Article history:
Received 24 April 2014
Received in revised form 27 August 2014
Accepted 22 October 2014
Available online 31 October 2014

Keywords:
Anti-fouling surfaces
Bacteriocidal activity
Charge density threshold
Killing efficiency
Charge clustering
Interfacial stress

ABSTRACT

This work examines how the antimicrobial (killing) activity of net-negative surfaces depends on the presentation of antimicrobial cationic functionality: distributed versus clustered, and flat clusters versus raised clusters. Specifically, the ability to kill *Staphylococcus aureus* by sparsely distributed 10 nm cationic nanoparticles, immobilized on a negative surface and backfilled with a PEG (polyethylene glycol) brush, was compared with that for a dense layer of the same immobilized nanoparticles. Additionally, sparsely distributed 10 nm poly-L-lysine (PLL) coils, adsorbed to a surface to produce flat cationic "patches" and backfilled with a PEG brush were compared to a saturated adsorbed layer of PLL. The latter resembled classical uniformly cationic antimicrobial surfaces. The protrusion of the cationic clusters substantially influenced killing but the surface concentration of the clusters had minor impact, as long as bacteria adhered. When surfaces were functionalized at the minimum nanoparticle and patch densities needed for bacterial adhesion, killing activity was substantial within 30 min and nearly complete within 2 h. Essentially identical killing was observed on more densely functionalized surfaces. Surfaces containing protruding (by about 8 nm) nanoparticles accomplished rapid killing (at 30 min) compared with surfaces containing similarly cationic but flat features (PLL patches). Importantly, the overall surface density of cationic functionality within the clusters was lower than reported thresholds for antimicrobial action. Also surprising, the nanoparticles were far more deadly when surface-immobilized compared with free in solution. These findings support a killing mechanism involving interfacial stress.

1. Introduction

The quest for antimicrobial materials has diverged into two strategies: Antimicrobial compounds are either leached from a material or their surfaces are rendered bacteriocidal. Indiscriminate leaching of biocides into large volumes of fluid is wasteful and lowers overall efficiency [1,2]. Conversely, antimicrobial surfaces kill only the bacteria which come into intimate contact. For surfaces with an established correlation between adhesion and killing activity [3,4], fouling reduces their effectiveness [5,6]. Cationic surfaces exemplify this behavior, possessing contact-killing properties [5,7–11] but tending to retain, through electrostatic attractions, adherent bacteria [5]. A general design goal for contact-kill surfaces is the facile release of dead bacteria so that the active surface is constantly accessible to additional live bacteria. Deadly surfaces of low bacteria adhesion are therefore a design target.

Since cationic functionality is responsible for both bacterial killing and adhesive fouling [4], we pursued surface presentations of positive charge that minimize adhesion and maintain killing activity. The appropriate surface design is not obvious in the absence of universally accepted contact-kill mechanisms. One school of thought tethers killing moieties on polymer chains attached to a surface, to facilitate penetration of the bacterial membrane [10,12,13], similar to the solution-based mechanism. Membrane insertion on biocidal surfaces has not, however, been proven. In fact, there is mounting evidence that contact-killing can occur on surfaces whose functional groups cannot access the bacterial membrane (buried 50 nm or more within the bacterial envelope) [14–17]. These surfaces include amine-functionalized self-assembled monolayers [18] and layer-by-layer structures [19,20]. Efficient killing by high molecular weight polycationic brushes allows for polycation chains insertion into the

* Corresponding author. Tel.: +1 413 577 1417; fax: +1 413 577 0946.
E-mail address: Santore@mail.pse.umass.edu (M.M. Santore).

http://dx.doi.org/10.1016/j.colsurfb.2014.10.043
0927-7765/

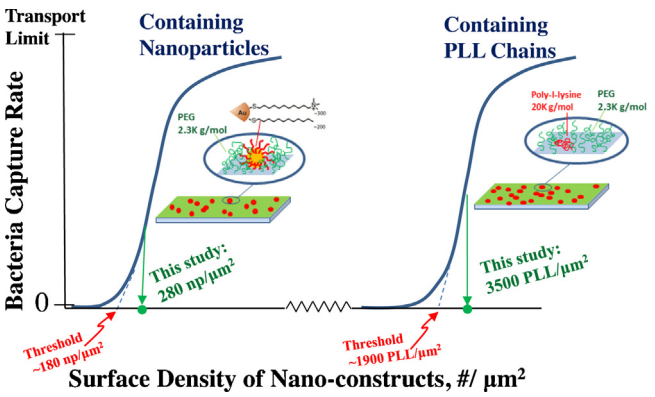

Fig. 1. General schematic of the surface structure and the influence of surface composition on the capture rates of flowing *S. aureus* cells onto PEG brush surfaces containing adhesive nanoconstructs. Thresholds are indicated quantitatively for the particular types of PEG brush and nanoconstructs in the current work. These threshold surface loadings for each type of nanoconstruct motivate the choice of the surface loadings of nanoconstructs in this study of antimicrobial activity. Notably, at the surface loadings of nanoparticles and PLL studied here, the bacterial capture rates are well below the transport-limit.

bacterial membrane [5,21]; however, the killing with lower molecular weight polycation brushes argues against the necessity of membrane penetration [5,21]. An alternate hypothesis involves ion exchange and release of multivalent cations from the bacterial membrane in the region where the bacterial cell contacts a cationic surface [22]. More recently, mechanisms involving deadly interfacial forces have been proposed [4,23,24]. Despite the lack of clarity on the mechanism, it is generally accepted that killing requires (cationic) surface charge densities exceeding a threshold of $1–5 \times 10^{15}$ [21] or $10^{12}–10^{16}$ [22] amines/cm^2 depending on the bacteria.

Zydrko et al. [25] employed surface brushes containing both cationic and sterically repulsive PEG (polyethylene glycol) chains to tune bacterial capture. Li et al. [26] demonstrated that surfaces with nanoscale roughness captured bacteria more efficiently than flat surfaces of similar chemistry. Neither study investigated killing.

To facilitate tunable bacterial adhesion, our lab developed PEG brush surfaces containing embedded cationic nanoparticles [27] or cationic polyelectrolyte chains [28], which we refer to here as cationic "nanoconstructs". The cationic nanoparticles and poly-L-lysine (PLL) chains contained similar cationic content, 200 amines/nanoparticle and 130 amines/PLL chain; however, immobilized nanoparticles protruded on the order of 10 nm from the substrate while adsorbed PLL coils lay relatively flat (within 1–2 nm) to the substrate, detailed below. Our PEG brush surface architectures, in the absence of embedded cationic nanoconstructs, resisted protein adsorption [29,30] and were non-adhesive for *Staphylococcus aureus* on timescales of interest [27,31]. This ensured that, on the test surfaces containing both the nanoconstructs and the PEG brush, bacteria were retained only through adhesion to the nanoconstructs. Indeed, *S. aureus* adhered only on surfaces whose densities of nanoconstructs exceeded a distinct threshold, shown schematically in Fig. 1 [27,28]. With bacterial adhesion well characterized on these surfaces, the current paper examines their bacteriocidal activity. The current study focuses on the least adhesive surfaces still able to capture and hold substantial numbers of bacteria in gentle flow. Worth noting, partial to near-complete bacterial release from these surfaces was previously documented [32].

The current study focuses on two test surface designs from previous libraries: A test surface with a low cationic nanoparticle density (280 nanoparticles/μm^2) and a test surface with a low PLL patch density (3500 patches/μm^2), both backfilled with a non-adhesive PEG brush. Both test surfaces are benchmarked against control surfaces containing dense loadings of the corresponding cationic nanoconstructs. The two sparsely-loaded test surfaces each contain the minimum respective nanoconstruct densities needed to capture and retain substantial numbers of flowing *S. aureus*, indicated in Fig. 1. (Fig. 1 is a schematic representation of prior results for bacterial capture [27,28], and motivates the specific surface compositions employed here.) The large differences in the adhesion thresholds in Fig. 1 resulted from the differences in the nanoparticle protrusion relative to the brush. Thus the two test surfaces in this study have very different nanoconstruct densities. Prior work, using shear flow chambers, established relatively weak bacterial adhesion on these test surfaces. For instance, 90% of captured *S. aureus* could be rinsed from the sparse nanoparticle surface with 13 pN shearing force, even 30 min after bacterial capture [32].

In addition to comparing the killing activity of different surfaces, this paper also compares the surface activity of immobilized cationic nanoparticles to that in free solution. Immobilized nanoparticles were fundamentally more deadly than free nanoparticles in buffer or growth medium.

2. Materials and methods

2.1. Nanoparticles and polymers

Cationically functionalized gold nanoparticles were synthesized according to standard methods [33]. Characterization by TEM indicated a 7 nm core, and an overall diameter of 11 nm. The ligand shell contained ~200 cationic ligands (N,N-trimethyl(11 mercaptoundecyl) ammonium chloride) and 300 hydrophobic (1-mercaptoundane) ligands.

Poly-L-lysine (PLL), of nominal molecular weight 20,000 g/mol, was purchased from Sigma–Aldrich (catalog number P7890, M_v in the range 15,000–30,000 g/mol) and used directly to create cationic surface regions. The same PLL was modified by the attachment of 2300 g/mol-molecular weight polyethylene glycol (PEG) chains to produce a PLL-PEG graft copolymer for the surface brush. We targeted functionalization of about one third of the amines on the PLL, based on reports [29,31] and our own confirmation [32] that a copolymer of this composition, when adsorbed on negative surfaces, prevents bacteria and protein adsorption by formation of a PEG brush. Copolymer synthesis followed published methods [29,30]. The composition of the graft copolymer was assessed by ^{1}H NMR in D_2O using a Bruker 400 mHz instrument. Comparison of the lysine side chain peak at 2.909 ppm and the PEG peak at 3.615 ppm revealed functionalization of 34% of the PLL amines.

2.2. Surface fabrication

Four surfaces, in Table 1, were studied. All were based on acid-etched microscope slides, soaked overnight in concentrated sulfuric acid and then rinsed in DI water. Onto this were deposited polymers and/or nanoparticles that were irreversibly physically bound (beyond the relevant timescales). Effectively permanent attachment of nanoparticles was confirmed [27,32] in a variety of conditions: rinsing in water and buffers between pH 5 and 8, drying, passing of an air bubble (3-phase contact line), addition of up to 5 M NaCl, organic solvents, sonication, and protein and sodium dodecylsulfate adsorption challenge. PLL retention was established at ionic strengths up to 1 M NaCl, and exposure to proteins and polymers [34].

Surfaces were prepared by placing each slide in a laminar flow chamber. DI water or pH 7.4 phosphate buffer flowed continuously at a wall shear rate of 10 s^{-1} over each surface and different nanoparticle and polymer solutions were introduced. A saturated PLL control surface was created by flowing a 5 ppm solution of PLL in phosphate buffer for 10 min followed by reinjection of the

Table 1
Characteristics of nanoconstructs and surfaces.

Nano-constructs	Nanoparticles: Height: 7–8 nm Diameter: 10 nm Zeta potential: 25 mV Number of amines: 200		Individual PLL chains: Height: flat (~1 nm) Diameter: 8 nm Zeta potential: 7 mV Number of amines: 130	
Surfaces	"Sparse nanoparticle"	"Dense nanoparticle"	"Sparse PLL"	"Saturated PLL"
Nanoparticle content	280/μm^2	1000/μm^2	–	–
PLL coil content	–	–	3500/μm^2	12,000/μm^2
PLL-PEG backfill, mg/m^2[a]	0.61	0.3	0.67	0.0
Avg spacing between cationic constructs, nm	60	32	17	–
Overall content of cationic groups, #/cm^2	5.6×10^{12}	2.0×10^{13}	8.7×10^{15}	3.1×10^{16}
S. aureus capture rate (for 2×10^6 cells/ml), cells/m^2 min	0.58×10^9	2.4×10^9	1.3×10^9	2.4×10^9
Zeta potential in buffer, mV (for $\kappa^{-1} = 2$ nm)[b]	-27 ± 3	-20 ± 3	-20 ± 3	6 ± 2

[a] PLL-PEG adsorbs at a level of 1.1 mg/m^2 on a bare silica surface.
[b] κ^{-1} is the Debye length. Also the zeta potential of our bare silica in this buffer is -73 ± 4 mV.

buffer. This flow time ensured surface saturation with 0.4 mg/m^2 PLL, confirmed by optical reflectometry [34].

Sparse PLL and nanoparticle-containing surfaces, along with a more densely functionalized nanoparticle surface were created in similar fashion. Timed flow of nanoparticles or PLL was followed by buffer reinjection to produce each targeted surface loading less than saturation. The remaining surface was then backfilled with a PEG brush by introducing a 100 ppm solution of PEG-PLL copolymer in phosphate buffer for 10 min. Flowing buffer was then reintroduced.

2.3. Surface characterization

The amounts of nanoparticles and polymers on each type of surface were measured by near-Brewster reflectometry as previously described [27,35]. Zeta potential measurements were made on a system in which the same amounts of polymer and nanoparticles were adsorbed on 1-μm silica spheres from Geltech (Orlando, FL). Dry substrates were characterized by AFM (Multimode AFM-2 with a Nanoscope IV scanning probe controller, Veeco, Inc.). Tapping mode with nominal spring constant of 42 N/m and nominal resonance frequency of 320 kHz was employed to determine the numbers and heights of deposited nanoparticles, with and without PLL-PEG backfill.

2.4. Bacteria

S. aureus bacteria (ATCC 25923) were grown, following standard procedures, in Mueller-Hinton (MH) medium, incubating aerobically overnight at 37 °C while shaking at 200 rpm. After 24 h, bacteria were harvested during logarithmic growth. To remove proteins and other free biomolecules, bacterial suspensions were centrifuged at 1000 × *g* and cells were re-suspended in phosphate buffer, a procedure which was conducted twice. Bacteria were stored at 4 °C and studied within 18 h. For some studies cells were re-suspended in MH broth after the second centrifugation and used immediately.

2.5. Bacteria capture from flow

Bacteria capture was conducted on a lateral microscope, oriented so that gravity did not influence the bacteria-surface interaction. Cells accumulated through adhesive interactions only. *S. aureus* cells, at a concentration of 2×10^6/ml in pH 7.4 phosphate buffer, were flowed over surfaces at a wall shear rate of 22 s^{-1} for 3 min, sufficient to capture at least 100 cells within the 240 μm × 180 μm field of view. Flow was then switched back to buffer for 3 min prior to viability studies.

2.6. Application of live-dead staining assay on surface-bound bacteria

We examined the viability of surface-bound bacteria using the Baclight Bacterial Viability Kit, L7012. It contained SYTO 9 and propidium iodide dyes that are usually applied to suspended bacteria. We were concerned, however, that removing bacteria from the surface could alter their viability, or that live or dead bacteria could be selectively removed and assayed [36]. We therefore applied the dyes directly to the adhered bacteria.

After opening the flow chamber, a drop of dye mixture was then applied to the test surface, and a cover slip placed on the surface. After at least 3 min the bacteria were examined on a Nikon Diaphot 300 fluorescence microscope, with a 40× fluorescence objective, employing filter cubes with 480 nm/500 nm and 580 nm/635 nm excitation/emission wavelengths for the green (SYTO 9) and red (propidium iodide) channels respectively. Bacteria appear green when alive and red when dead. While the shortest time at which bacterial viability could be assessed was a total of ~9 min surface residence time (the sum of a median 1.5 min residence during deposition, 3 min rinsing, a minute to open the chamber, and 3 min dye exposure), additional images were taken up to 2 h later to assess the killing kinetics. The 9 min bacteria residence time, with a 3 min dye exposure, proved sufficient for green and red dye color development with the *S. aureus*. For instance, on nonbacteriodical glass, adherent bacteria stained green by 3 min dye exposure and remained green. This control supports the significance of the color changes recorded on the test surfaces.

2.7. Control for live-dead staining assay of surface-bound bacteria

An additional control validated the application of the Baclight assay to surface-bound bacteria. Cells of *S. aureus* were captured from flow on a surface containing 1000 nanoparticles/μm^2 (having intermediate biocidal activity) and stained with the Baclight kit as described above. Next, 20 μL of liquid soft MH agar (6 g/L agar powder in MH broth) was applied to the bacteria and a cover slip was placed. Bacteria were incubated at 37 °C for up to 9 h and examined later to determine growth of initially adhered cells. It was found (data in the Supporting Information) that captured bacteria that stained red on the surface did not grow into colonies but remained as single adherent cells; however, many bacteria that stained green could be seen, in time, to grow on the surface. Some cells, originally

staining green, did not grow because they died later, as would be expected for a surface with intermediate killing activity. This control substantiated the use of the Baclight kit assay for surface-bound bacteria. This exercise supports the interpretation that the fraction of red cells, especially at short times, represents a lower bound on killing, and a conservative estimate of the biocidal surface property. Some cells destined for death may have not yet stained red; however, all red cells were non-propagating.

2.8. Optical density assay for MIC in solution

Freshly prepared *S. aureus* cells were diluted into MH broth at a concentration ($\sim 10^5$ cells/ml) to produce an optical density of 0.001 at a wavelength of 600 nm in a CECIL C3041 UV–vis spectrophotometer. Different amounts of cationic nanoparticles, on the order of a few microliters of a concentrated stock solution in deionized water, were mixed with milliliter-sized quantities of bacterial suspensions to make serial dilutions of the nanoparticle dosage. After measurements of the initial optical density of each mixture, the suspensions were incubated for 6 h at 37 °C. Then they were sonicated in a VWR Aquasonic 75HT sonicator bath for 60 min to re-suspend aggregated bacteria, the optical density was again measured. Optical density tests for the MIC were run three times with different batches of *S. aureus* cells.

2.9. Application of live-dead staining assay in solution

Studies of nanoparticle killing in solution employed a 500 ppm nanoparticle suspension and varied the bacteria concentration. Nanoparticles and bacteria were mixed at the desired concentrations in pH 7.4 phosphate buffer for 4 h at room temperature. The suspension was then sonicated for 1 h to disrupt aggregates and the Baclight dye mixture added. After further incubation for 10 min, 5 μL of the stained mixture was placed on a microscope slide and a coverslip added. Fluorescence microscopy images at 40× were obtained as described above. Adequate bacterial staining was observed in the presence of 10 mM phosphate buffer. Live bacteria stained green while suspensions into which ethanol was added stained red, arguing that phosphate buffer was tolerated by the dyes with these *S. aureus*.

2.10. Control for influence of sonication on bacteria viability

Freshly prepared bacteria in MH broth were diluted to 10^3/ml in MH broth and samples were sonicated serially for 0, 2, 10, 30 and 60 min. Colony forming unit assays revealed no influence of sonication.

2.11. Colony-forming unit assay

We followed a standard procedure: 100 μL of bacterial suspension diluted to 10^3 cells/ml in MH broth was spread on an MH-agar plate using a sterile applicator. The covered agar plate was incubated aerobically at 37 °C for 18 h and colonies were counted.

3. Results

3.1. Surface characterization

Important features of the surfaces in this work include their net negative charge and the clustered presentation of cationic functionality, along with its position relative to the substrate and the hydrated polymer brush. Table 1 summarizes the surface compositions and zeta potentials of the various surfaces. The net negative zeta potential of the sparse surfaces, despite the positive charge on the nanoparticles and PLL chains argues that, on the sparse surfaces, positive interfacial charge is localized at the positions of the immobilized nano-constructs, as expected. The net negative charge of the sparse surfaces distinguishes them from typical uniformly cationic antimicrobial surfaces exemplified by the saturated PLL layer.

The surface topography of the dry nanoparticle surfaces is revealed in AFM micrographs in Fig. 2, before and after backfilling with PLL-PEG copolymer. The micrographs show the random positioning of the nanoparticles and support the previous observation, using near-Brewster reflectometry to probe larger surface areas, that nanoparticles are not removed by the backfilling process [27]. In Fig. 2, the dry heights of the immobilized nanoparticles slightly exceed 8 nm, as AFM is sensitive to the gold cores and may deform the ligand shells. After backfilling with the PLL-PEG brush and drying, the nanoparticle heights appear about a nanometer shorter, because the PLL-PEG is deposited onto the microscope slide and not on the particles. In water, the PEG brushes swell to about 8 nanometers, a calculated estimate [35]. (Solvated brush heights cannot be determined by AFM due to the dilute character of the brush.) Thus, parts of the nanoparticles are near the wet brush periphery.

On surfaces containing sparse PLL patches or PLL patches backfilled with a PLL-PEG brush, the PLL patches themselves are quite flat, especially compared with the nanoparticle-containing surfaces. Polyelectrolytes such as PLL, adsorbed on oppositely charged surfaces at moderate ionic strengths, assume flat conformations at the liquid–solid interface, especially at low coverages when adsorbed chains are isolated [37,38]. This flatness is confirmed by dynamic light scattering in the Supporting Information. Data show that the hydrodynamic radii of silica particles containing adsorbed PLL are similar to those of bare particles. Additionally, single-photon fluorescence microscopy studies revealed the random non-aggregated arrangement of adsorbed PLL chains [35]. From these characterization studies evolves a picture of flat PLL patches embedded within a PLL-PEG brush. We estimate the in-plane diameter of the adsorbed PLL chains from the 8 nm coil diameter from dynamic light scattering.

3.2. Bacterial toxicity

For different times after *S. aureus* cells were captured, the bacteriocidal activity of 4 different surfaces was compared: sparse ($280/\mu m^2$) and dense ($1000/\mu m^2$) immobilized nanoparticles versus sparse ($3500/\mu m^2$) and saturated ($12{,}000/\mu m^2$) PLL coils. Fig. 3 summarizes the average killing kinetics for three different surfaces of each type, studied with two different batches of *S. aureus* bacteria. Additionally, the Supporting Information contains example micrographs for bacteria on each type of surface at different surface residence times. The Supporting Information also includes example data for bacteria capture kinetics and retention in flow. In Fig. 3, the bacteria residence times (defined as the time from the midpoint of the deposition process to the time of examination) vary from 9 min to 2 h.

Fig. 3 shows that bacteria start to die once they are captured on the surfaces and are substantially dead within 2 h. The ultimate extent of killing and the kinetics depend on the surface design. Worth noting, live-dead stain controls with each batch of bacteria indicated live cells in excess of 99% prior to capture.

Fig. 3 makes several important points. First, substantial killing, up to 40% in the case of the dense nanoparticles, occurs within the first 9 min of bacterial contact with the surface. Second, killing efficiency is not proportional to cationic functionality: Sparsely loaded cationic surfaces, if they contain enough cationic functionality to adhere bacteria, are fairly effective at killing bacteria. Compared with sparsely loaded cationic clusters, similar or slightly greater killing is obtained for the maximum cationic loading of

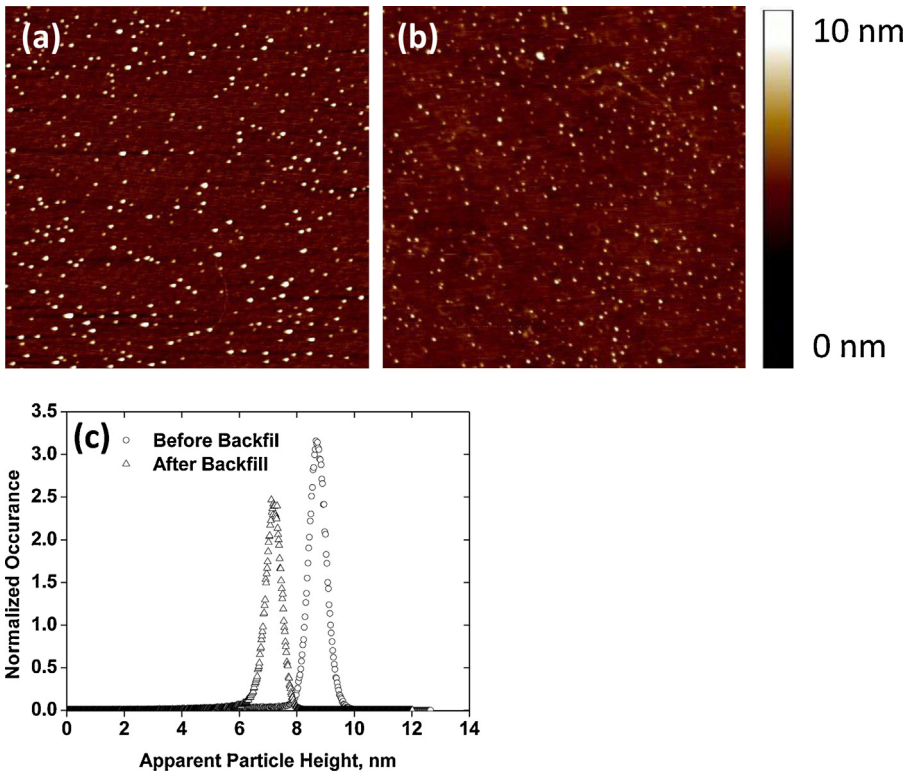

Fig. 2. AFM images (2 μm × 2 μm) of two different surfaces having 100 nanoparticles/μm^2 (a) before (b) and after backfilling with PLL-PEG. The particle density is unaffected by backfilling. (c) The histogram of particle heights shows that the apparent particle height decreases from 8.6 to 7.2 nm, upon backfilling. Normalization of peak area is based on 100% total.

each type. Finally and most importantly, at intermediate times, the nanoparticle-containing surfaces kill *S. aureus* far better than do the PLL-containing surfaces.

Controls associated with Fig. 3 include bacteria adhered to acid-etched glass microscope slides from flow and bacteria allowed to settle under gravity (since *S. aureus* cells cannot be adhesively captured) on PLL-PEG layers not containing cationic nanoconstructs. In these controls, the bacteria remain viable. This argues that the killing activity on surfaces containing the adhesive nanoconstructs is a result of the presence of the PLL patches or cationic nanoparticles on the test surfaces. Worth emphasizing, while PLL chains anchor the PLL-PEG copolymer to the substrates when a PEG brush is present, this PLL is buried beneath the brush, anchored electrostatically to the glass substrate, and lower in cationic charge density

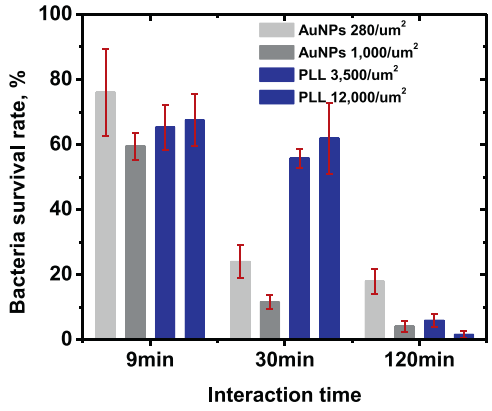

Fig. 3. Survival rates of *S. aureus* captured from flow, at a wall shear rate of 22 s^{-1}, on surfaces containing nanoparticles or PLL coils, indicated. Error bars represent a standard deviation. Five images were taken at 9 and 120 min for each surface type. Three images were taken at 30 min for each surface type.

than the PLL homopolymer making up the patches. As part of the anchors for the PEG brushes, the PLL part of the PLL-PEG copolymer does not adhere or kill bacteria.

3.3. Surface versus bulk solution killing

While we expect surfaces containing immobilized nanoparticles to kill bacteria more efficiently than the same nanoparticles leached indiscriminately into solution (which may never reach bacteria), we address here the relative killing efficiency of free and immobilized nanoparticles. This study was designed to ensure that nanoparticles in solution reached the bacterial surfaces in substantial numbers.

Fig. 4 presents the results of a classical optical density assay for the minimum inhibitory concentration of nanoparticles in solution. In this assay, varied amounts of nanoparticles were added to a MH broth containing 10^5/ml *S. aureus* (having an optical density, without nanoparticles of OD_{600} = 0.001). The optical density of the suspension, after 6 h of incubation at 37 °C (to allow bacteria to propagate), is classically taken as an indicator of the MIC. A high optical density indicates that bacteria have multiplied in the 6 h growth period, and a low optical density indicates bacteriocidal activity, or at least inhibition of growth. Following this approach, Fig. 4 suggests an *apparent* MIC of 100 ppm for the cationic nanoparticles against *S. aureus*.

While the optical density method is well accepted for molecular antimicrobials, it is inconclusive for nanoparticle suspensions such as ours for two reasons. First adsorption of the nanoparticles on the bacteria causes their aggregation, with bacteria-nanoparticle sediments evident in the inset of Fig. 4. These sediments deplete bacteria from the main suspension, reducing optical density as an artifact. However, even when bacteria were re-suspended by mixing or by up to 60 min of sonication (which we tested to ensure that it did not affect bacterial viability) the optical density of the suspension after 6 h was always much lower than its initial level. A second

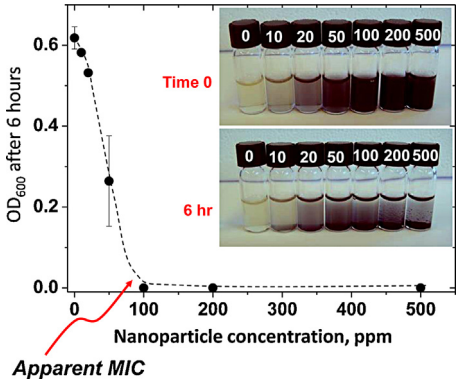

Fig. 4. Classical assay to determine the solution-phase MIC of the nanoparticles based on optical density at 600 nm. The upper row of vials was photographed immediately after mixing: the contents were 10^5/ml *S. aureus* and the nanoparticle concentrations indicated on the lids, ppm. Also evident in the upper images is the color intensity of the nanoparticles at different concentrations. The lower row of vials, after 6 h at 37 °C, indicates aggregation of the nanoparticles and bacteria, with nearly all the nanoparticles associated with the settled bacteria. Comparison of the color supernatants after 6 h to the upper row suggests the final free nanoparticle concentrations, in all cases, is less than 50 ppm.

problem with the optical density method stems from the standard procedure of using reference solutions comprised of antimicrobial compound (in this case nanoparticles) at each concentration of interest. It was difficult to assess suspended bacteria concentrations because nanoparticle concentrations exceeding ~50 ppm were strongly absorbing at 600 nm, dominating signal from bacteria.

While the optical density study was inconclusive for the purposes of determining bacteria viability or the MIC, we keep it in this report to document when a standard method is inappropriate. Further, Fig. 4 provides insight into bacteria-nanoparticle interactions in suspension: the images clearly demonstrate the flocculation of the bacteria by adhesion to the nanoparticles. This is significant because, with 95% of the nanoparticles located in bacterial aggregate sediment (an estimate which stems from a visual comparison of supernatant color after 6 h to that of the initial solutions), *we can be certain that the nanoparticles adhered to the bacterial surfaces*. The removal of bacteria from the suspension in the presence of nanoparticles was also confirmed by light microscopic observation. Nanoparticles in the absence of bacteria did not settle. Further, we assert that this adhesion/adsorption process occurred in the presence of growth medium, demonstrating that the medium did not interfere with the nanoparticle adhesion to bacteria.

These complexities necessitated other methods to assess nanoparticle killing activity in solution. Using a standard CFU (colony forming unit) assay, we assessed the viability of *S. aureus* (10^5/ml), incubated at 37 °C for 6 h in MH broth with 500 ppm nanoparticles. Figure SI-5 in the Supporting Information demonstrates that agar plates inoculated with a nanoparticle-bacteria suspension, diluted to 10^3 cells/ml (based on the original microscopic count), show substantial colony growth and, with live dead staining, nearly no killing. The colony numbers and viability are similar to a bacterial suspension of the same concentration without nanoparticles. These results, combined with the observations in Fig. 4, argue that in the presence of MH broth, *S. aureus* are not substantially killed by up to 500 ppm nanoparticles though the nanoparticles adhere substantially to bacteria.

We considered the possibility that interaction of the growth medium inhibited the nanoparticle's killing action. Another possibility is that bacteria are more readily killed in buffer (like conditions for the surface studies of Fig. 3) than they are in MH broth. To address both possibilities, we studied the solution-phase killing action of 500 ppm nanoparticles on *S. aureus* bacteria in phosphate buffer, summarized in Table 2. The overall nanoparticle concentration was fixed at 500 ppm, and the bacteria concentration was varied from 10^5 to 10^8/ml to vary the nanoparticle/bacteria ratio. Nanoparticle-bacteria aggregation was apparent shortly after mixing. By 4 h, nearly complete settling of bacteria had occurred. In the cases with the greatest bacteria concentrations, this completely removed the nanoparticles from the supernatant, indicating adhesion of all nanoparticles onto the bacteria. With fewer bacteria dosed with the nanoparticles, however, the presence of excess nanoparticles suspended in solution suggested that the settled bacteria were already saturated with nanoparticles. The panels of the figure list the estimated numbers of nanoparticles per original bacterium.

The viability of the suspension-phase (or aggregated) bacteria was studied in Table 2 by live-dead staining as shown. Nearly all bacteria are living, despite exposure to and contact with large numbers of nanoparticles. Large numbers of viable bacteria were additionally confirmed by CFU. Of note with 10^5 bacteria/ml, the bacteria were too sparse to be reliably visualized with live-dead staining. Therefore, additionally, in the Supporting Information, the CFU method revealed substantial bacteria viability, rivaling that without nanoparticles.

4. Discussion

The experimental results provide new insights into strategic surface designs for effective contact-bacterial-kill surfaces and additionally provide new perspectives about potential surface-killing mechanisms. Importantly, when considered with our previous adhesion studies involving bacteria on related surfaces [27,32], these data suggest that clustering of cationic functionality facilitates bacterial killing on minimally adhesive bacteria-capture surfaces.

4.1. Surface designs: cation density and the role of clustered distribution

We report substantial killing of *S. aureus* bacteria on surfaces having relatively small overall cationic charge densities compared with the literature: 5.6×10^{12}/cm^2 on our sparse nanoparticle surfaces and 10^{16}/cm^2 on our patchy PLL surfaces. As some of the cationic functionality lies beneath nanoparticles, on the nanoparticle-containing surfaces, these values represent an upper limit on what might be accessible to bacteria, by perhaps 50%. By comparison, the minimum charge density in the literature for contact killing of *Staphylococcus epidermidis* is 10^{14}–10^{16} cationic charges/cm^2 [22]. Particularly interesting, the killing activity of our surfaces is not much improved by increasing the surface loadings of either type of cationic nanoconstruct.

Clustered cationic organization is critical to good contact-killing efficiency on these surfaces. Uniform distribution of the same cationic functionality would produce surfaces entirely non-adhesive to bacteria (like the PEO-PLL control surface) and therefore not antimicrobial [27]. With capture facilitated by charge clustering on otherwise non-adhesive surfaces, clustered functionality facilitates a chance at killing which would not occur on uniform surfaces of the same cationic density.

Strong evidence suggests that the contact region between each bacterium and the surface contains both nanoparticles (or PLL coils) and PEG brush, and that the contact region is not comprised mostly, or entirely, of cationic species. This is an important distinction because we have asserted that our surfaces are fundamentally different from uniform cationic surfaces both in terms of net charge

Table 2
Mixing S. aureus with 500 ppm nanoparticles in buffer.

Bacteria concentration	Appearance		Viability image Live/dead stain on drop of suspension
	Initial	4 h	
10^5 cells/ml 1.6×10^9 np avail/cell 1.5×10^7 np adh'd/orig cell			
10^6 cells/ml 1.6×10^8 np avail/cell 1.5×10^7 np adh'd/orig cell			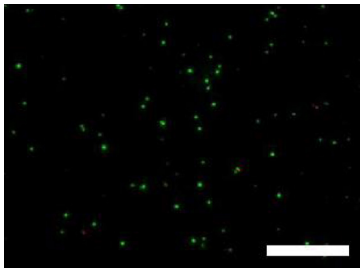
10^7 cells/ml 1.6×10^7 np avail/cell 1.5×10^7 np adh'd/orig cell			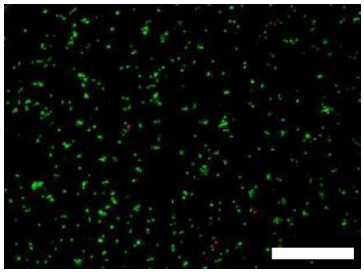
10^8 cells/ml 1.6×10^6 np avail/cell 1.6×10^6 np adh'd/orig cell		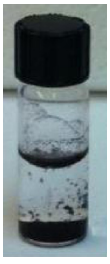	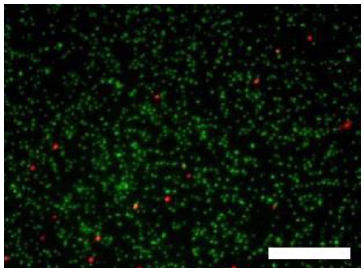

The scale bars are 50 μm.

(zeta potential) and local clustering of cationic charge. The alternate possibility, which we argue is not the case, is that the nanoparticles or PLL are themselves greatly clustered so that bacteria adsorb to regions populated largely or exclusively by these cationic nanoconstructs. In the latter case, the bacteria-surface contact zone would resemble the uniform control surfaces.

Three arguments refute the latter possibility. First is the experimental observation of randomly distributed cationic nanoconstructs. The AFM images of the cationic nanoparticles in Fig. 2, along with previously published characterization of the adsorbed PLL distributions [35], include no instances of aggregates of nanoparticles or PLL which would comprise a locally uniform cationic region. Such aggregates would need to be prevalent in order to produce the relatively uniform bacteriocidal (or not) behaviors over hundreds of square microns, detailed in Figures SI-4 and 5. Second, bacterial adhesion on the sparse surfaces was dramatically weaker and more reversible than that on the uniform PLL and concentrated nanoparticle surfaces [32]. The surface regions in contact with bacterial cells were therefore fundamentally different on sparse and control surfaces. Finally, calculations support the high improbability, given random distributions of adhesive nanoconstructs [35], of finding regions appropriately sized for individual cell contact, containing high numbers of nanoconstructs.

For instance given randomly distributed nanoparticles (a Poisson distribution) having an *average* surface loading of 280 np/μm^2, the normalized probability of finding a half micron squared area (an estimate for the ultimate size of the bacteria-surface contact) containing 200 nanoparticles is miniscule: $\sim 10^{-37}$. Adherent bacteria therefore, experience nanoconstructs and substantial PEG brush together on the surface regions where they come to rest, though the local nanoconstruct concentration likely exceeds the average or "macroscopic" loading.

4.2. Raised versus flat clusters: killing kinetics and implications for mechanism

Our results demonstrate that, compared with flat PLL patches, raised presentation of clustered cationic functionality, by just a few nanometers, dramatically expedites *S. aureus* killing. These observations provide new design considerations for applications requiring fast-acting surfaces. The report by Madkour et al. is the only other work of which we are aware where *S. aureus* appear to be killed more quickly, within 5 min [5]. In that study, however, bacteria are removed from the antimicrobial surface and tested later for viability. They were found to be killed as a result of 5 min adhesive contact, but it is not clear if the stress (and tearing?) of removal influenced the results.

Regarding the killing mechanism, neither the flat nor protruding cationic nanoconstructs in this work are expected to penetrate the 20–40 nm thick cell envelope of *S. aureus* [14] to access the bacterial membrane. However, the slight protrusion of the nanoparticles seems an advantage: Fewer nanoparticles, compared with PLL patches of similar overall charge, are able to capture and kill *S. aureus*. The key may be accessibility to bacteria through the PEG surface brush, or it may be that slight penetration (on the order of nm) of the nanoparticles into the outer regions of the *S. aureus* envelope somehow affords greater killing effectiveness, perhaps by reaching structures where ion exchange is more lethal.

4.3. Free versus surface-immobilized nanoparticles: implications for killing mechanism

Important to our understanding of the contact-killing mechanism is the observed bacterial survival in nanoparticle solutions. The lack of nanoparticle activity against *S. aureus* is consistent with previous reports of *Escherichia coli* survival when exposed to suspended cationic nanoparticles [39]. In the current investigation, the removal of the nanoparticles from the supernatant when bacteria settled provided an assurance of the adhesion of the nanoparticles to the bacteria, with at least 10^6 np/initial bacterial cell (continued bacterial growth would reduce this number substantially). The initial appearance of aggregation at short times (<30 min, though setting of the sediment took longer) provided evidence that nanoparticles were afforded sufficient interaction times to contact bacteria. Yet these *S. aureus* were found to be predominantly viable after 4 h. Placement of the same nanoparticles on a sterically repulsive surface produced a material that killed bacteria substantially within 30 min and more extensively within 2 h. Worth noting, the numbers of nanoparticles adhered to the suspended bacteria was considerably greater than those available on the surface to reach each bacterium, yet the latter were more deadly.

Our results demonstrate that neither the cationic nanoparticles alone nor a PEG surface brush alone will kill *S. aureus*. Killing results, however, from the combined action of cationic nanoparticles and the sterically repulsive "non-interacting surface" or the nanoparticle immobilization. Possible mechanisms involve stresses that deform the bacteria on large scales (like droplet spreading) or that locally disrupt the organization of bacteria structures where the bacteria contacts the substrate, as has been discussed recently [23,24]. Another point worth pondering: The sparse nanoparticle surfaces are deadly, even though the surfaces touch bacteria only on a small portion of the overall bacterial surface. By contrast, antimicrobial compounds added to a bacterial suspension attack the cell on all sides. We find the contact-kill mechanism an intriguing puzzle, but our results indicate that very little contact is needed, the cell membrane need not be directly involved, and adhesive binding and local interactions can produce a global effect.

5. Conclusions

We present here a class of contact-kill antimicrobial surfaces, based on 10-nm clusters of cationic charge embedded in a sterically repulsive polyethylene glycol brush. These materials exhibit counterintuitive killing action against *S. aureus*. First, compared with the literature on non-leaching cationic contact antimicrobial surfaces, our surfaces are net negative (compared with positive surfaces in the literature). Our surfaces kill with extremely small densities of cationic functionality, below the previously reported minimum for antimicrobial action. Increased surface loading of the cationic nanoconstructs minimally improves killing. *S. aureus* contact with the sparse surfaces in this study involves a limited number of points corresponding to the nanoparticles or PLL nanoconstructs. In this way the effective killing interaction, were it to correspond only to the cationic functionality, is smaller than the overall bacteria-surface contact area.

The low density of cationic functionality is an advantage because it produces weaker bacteria adhesion and potential re-use of the surface. Indeed, the sparsely cationic surfaces were just above the minimum cationic functionality needed for bacterial capture. More uniform distribution of the same cationic charge would not have captured bacteria, clarifying the role of clustering in adhesion and killing. Clustering enables strong (relative to hydrodynamic forces) interactions between the bacteria and the surface, increasing bacterial retention and contact time, facilitating killing.

Further, we demonstrate substantial differences in killing kinetics between immobilized nanoparticles and flat cationic PLL patches. The immobilized nanoparticles accomplished substantial killing of *S. aureus* within 30 min, compared with slower killing kinetics by PLL coils that contain greater numbers of cationic groups. The difference might be a result of the protruding and more readily accessible functionality on the nanoparticles.

Most remarkably, we demonstrate that the immobilized cationic nanoparticles are deadly to *S. aureus* but do not substantially kill bacteria in solution. This suggests that the surface killing mechanism involves localized opposition of attractive and repulsive forces or, at the very least, a lack of movement of the nanoparticles, during their interactions with bacteria.

Acknowledgments

This work was supported by NSF 1264855, 1025020, and NIH R21 CA159109-01A1.

Appendix A. Supplementary data

Supplementary data associated with this article can be found, in the online version, at http://dx.doi.org/10.1016/j.colsurfb.2014.10.043.

References

[1] D.M. Yebra, S. Kiil, K. Dam-Johansen, Antifouling technology – past, present and future steps towards efficient and environmentally friendly antifouling coatings, Prog. Org. Coat. 50 (2004) 75.
[2] J. Heidler, A. Sapkota, R.U. Halden, Partitioning, persistence, and accumulation in digested sludge of the topical antiseptic triclocarban during wastewater treatment, Environ. Sci. Technol. 40 (2006) 3634.
[3] J. Strauss, A. Kadilak, C. Cronin, C.M. Mello, T.A. Camesano, Binding, inactivation, and adhesion forces between antimicrobial peptide cecropin P1 and pathogenic *E. coli*, Colloids Surf. B 75 (2010) 156.
[4] Y. Liu, J. Strauss, T.A. Camesano, Adhesion forces between *Staphylococcus epidermidis* and surfaces bearing self-assembled monolayers in the presence of model proteins, Biomaterials 29 (2008) 4374.
[5] A.E. Madkour, J.A. Dabkowski, K. Nusslein, G.N. Tew, Fast disinfecting antimicrobial surfaces, Langmuir 25 (2009) 1060.
[6] X. Xie, J. Moller, R. Konradi, M. Kisielow, A. Franco-Obregon, E. Nyfeler, A. Muhlebach, M. Chabria, M. Textor, Z.H. Lu, E. Reimhult, Automated time-resolved

analysis of bacteria-substrate interactions using functionalized microparticles and flow cytometry, Biomaterials 32 (2011) 4347.
[7] P. Gilbert, L.E. Moore, Cationic antisepsis: diversity of action under a common epithet, J. Appl. Microbiol. 99 (2005) 703.
[8] T. Ikeda, H. Hirayama, H. Yamaguchi, S. Tazuke, M. Watanabe, Polycationic biocides with pendant active groups – molecular-weight dependence of antibacterial activity, Antimicrob. Agents Chemother. 30 (1986) 132.
[9] T. Ikeda, H. Yamaguchi, S. Tazuke, New polymeric biocides – synthesis and antibacterial activities of polycations with pendant biguanide groups, Antimicrob. Agents Chemother. 26 (1984) 139.
[10] N.M. Milovic, J. Wang, K. Lewis, A.M. Klibanov, Immobilized N-alkylated polyethylenimine avidly kills bacteria by rupturing cell membranes with no resistance developed, Biotechnol. Bioeng. 90 (2005) 715.
[11] J.C. Tiller, S.B. Lee, K. Lewis, A.M. Klibanov, Polymer surfaces derivatized with poly(vinyl-N-hexylpyridinium) kill airborne and waterborne bacteria, Biotechnol. Bioeng. 79 (2002) 465.
[12] F. Costa, I.F. Carvalho, R.C. Montelaro, P. Gomes, M.C.L. Martins, Covalent immobilization of antimicrobial peptides (AMPs) onto biomaterial surfaces, Acta Biomater. 7 (2011) 1431.
[13] S.A. Onaizi, S.S.J. Leong, Tethering antimicrobial peptides: current status and potential challenges, Biotechnol. Adv. 29 (2011) 67.
[14] B.A. Dmitriev, F.V. Toukach, K.M. Schaper, O. Holst, E.T. Rietschel, S. Ehlers, Tertiary structure of bacterial murein: the scaffold model, J. Bacteriol. 185 (2003) 3458.
[15] V.R.F. Matias, A. Al-Amoudi, J. Dubochet, T.J. Beveridge, Cryo-transmission electron microscopy of frozen-hydrated sections of *Escherichia coli* and *Pseudomonas aeruginosa*, J. Bacteriol. 185 (2003) 6112.
[16] V.R.F. Matias, T.J. Beveridge, Cryo-electron microscopy reveals native polymeric cell wall structure in *Bacillus subtilis* 168 and the existence of a periplasmic space, Mol. Microbiol. 56 (2005) 240.
[17] S.O. Meroueh, K.Z. Bencze, D. Hesek, M. Lee, J.F. Fisher, T.L. Stemmler, S. Mobashery, Three-dimensional structure of the bacterial cell wall peptidoglycan, Proc. Natl. Acad. Sci. U. S. A. 103 (2006) 4404.
[18] A.J. Isquith, E.A. Abbott, P.A. Walters, Surface-bonded antimicrobial activity of an organosilicon quaternary ammonium chloride, Appl. Microbiol. 24 (1972) 859.
[19] J.A. Lichter, M.F. Rubner, Polyelectrolyte multilayers with intrinsic antimicrobial functionality: the importance of mobile polycations, Langmuir 25 (2009) 7686.
[20] S.Y. Wong, Q. Li, J. Veselinovic, B.S. Kim, A.M. Klibanov, P.T. Hammond, Bactericidal and virucidal ultrathin films assembled layer by layer from polycationic N-alkylated polyethylenimines and polyanions, Biomaterials 31 (2010) 4079.
[21] H. Murata, R.R. Koepsel, K. Matyjaszewski, A.J. Russell, Permanent, non-leaching antibacterial surfaces – 2: How high density cationic surfaces kill bacterial cells, Biomaterials 28 (2007) 4870.
[22] R. Kugler, O. Bouloussa, F. Rondelez, Evidence of a charge-density threshold for optimum efficiency of biocidal cationic surfaces, Microbiology 151 (2005) 1341.
[23] H.J. Busscher, H.C. van der Mei, How do bacteria know they are on a surface and regulate their response to an adhering state? PLoS Pathog. 8 (2012).
[24] L. Asri, M. Crismaru, S. Roest, Y. Chen, O. Ivashenko, P. Rudolf, J.C. Tiller, H.C. van der Mei, T.J.A. Loontjens, H.J. Busscher, A shape-adaptive, antibacterial-coating of immobilized quaternary-ammonium compounds tethered on hyperbranched polyurea and its mechanism of action, Adv. Funct. Mater. 24 (2014) 346.
[25] B. Zdyrko, V. Klep, X.W. Li, Q. Kang, S. Minko, X.J. Wen, I. Luzinov, Polymer brushes as active nanolayers for tunable bacteria adhesion, Mater. Sci. Eng. C 29 (2009) 680.
[26] X.Q. Li, T.Q. Liu, Y.T. Chen, The effects of the nanotopography of biomaterial surfaces on *Pseudomonas fluorescens* cell adhesion, Biochem. Eng. J. 22 (2004) 11.
[27] B. Fang, S. Gon, M. Park, K.N. Kumar, V.M. Rotello, K. Nusslein, M.M. Santore, Bacterial adhesion on hybrid cationic nanoparticle-polymer brush surfaces: ionic strength tunes capture from monovalent to multivalent binding, Colloids Surf. B 87 (2011) 109.
[28] S. Gon, K.N. Kumar, K. Nusslein, M.M. Santore, How bacteria adhere to brushy peg surfaces: clinging to flaws and compressing the brush, Macromolecules 45 (2012) 8373.
[29] N.P. Huang, R. Michel, J. Voros, M. Textor, R. Hofer, A. Rossi, D.L. Elbert, J.A. Hubbell, N.D. Spencer, Poly(L-lysine)-g-poly(ethylene glycol) layers on metal oxide surfaces: surface-analytical characterization and resistance to serum and fibrinogen adsorption, Langmuir 17 (2001) 489.
[30] G.L. Kenausis, J. Voros, D.L. Elbert, N.P. Huang, R. Hofer, L. Ruiz-Taylor, M. Textor, J.A. Hubbell, N.D. Spencer, Poly(L-lysine)-g-poly(ethylene glycol) layers on metal oxide surfaces: attachment mechanism and effects of polymer architecture on resistance to protein adsorption, J. Phys. Chem. B 104 (2000) 3298.
[31] L.G. Harris, S. Tosatti, M. Wieland, M. Textor, R.G. Richards, *Staphylococcus aureus* adhesion to titanium oxide surfaces coated with non-functionalized and peptide-functionalized poly(L-lysine)-grafted-poly(ethylene glycol) copolymers, Biomaterials 25 (2004) 4135.
[32] B. Fang, Y. Jiang, V.M. Rotello, K. Nusslein, M.M. Santore, Easy come easy go: surfaces containing immobilized nanoparticles or isolated polycation chains facilitate removal of captured *Staphylococcus aureus* by retarding bacterial bond maturation, ACS Nano 8 (2014) 1180.
[33] S. Srivastava, B. Samanta, B.J. Jordan, R. Hong, Q. Xiao, M.T. Tuominen, V.M. Rotello, Integrated magnetic bionanocomposites through nanoparticle-mediated assembly of ferritin, J. Am. Chem. Soc. 129 (2007) 11776.
[34] S. Gon, B. Fang, M.M. Santore, Interaction of cationic proteins and polypeptides with biocompatible cationically anchored PEG brushes, Macromolecules 44 (2011) 8161.
[35] S. Gon, M. Bendersky, J.L. Ross, M.M. Santore, Manipulating protein adsorption using a patchy protein-resistant brush, Langmuir 26 (2010) 12147.
[36] S. Pogodin, J. Hasan, V.A. Baulin, H.K. Webb, V.K. Truong, T.H.P. Nguyen, V. Boshkovikj, C.J. Fluke, G.S. Watson, J.A. Watson, R.J. Crawford, E.P. Ivanova, Biophysical model of bacterial cell interactions with nanopatterned cicada wing surfaces, Biophys. J. 104 (2013) 835.
[37] Y. Shin, J.E. Roberts, M.M. Santore, Influence of charge density and coverage on bound fraction for a weakly cationic polyelectrolyte adsorbing onto silica, Macromolecules 35 (2002) 4090.
[38] G. Fleer, M.A. Cohen Stuart, J.M.H.M. Scheutjens, T. Cosgrove, B. Vincent, Polymers at Interfaces, Chapman and Hall, London, 1993.
[39] C.M. Goodman, C.D. McCusker, T. Yilmaz, V.M. Rotello, Toxicity of gold nanoparticles functionalized with cationic and anionic side chains, Bioconjugate Chem. 15 (2004) 897.